Improvement of InGaAs/GaAs vertical-cavity surface-emitting lasers by post-oxidation annealing

Changling Yan (晏长岭)*, Yun Deng (邓 昀), Peng Li (李 鹏), Xiaomao Song (宋小卯), and Jianwei Shi (史建伟)

National Key Lab on High-Power Semiconductor Lasers, Changchun University of Science and Technology, Changchun 130022, China

**Corresponding author: changling_yan@yahoo.com.cn*

Received April 27, 2012; accepted July 10, 2012; posted online October 24, 2012

InGaAs/GaAs vertical-cavity surface-emitting lasers (VCSELs) are fabricated by a thermal selective wet-oxidation confinement technique. Post-oxidation annealing in a nitrogen environment at high temperatures is then conducted to improve the performance of the oxide-confined InGaAs/GaAs VCSELs. The optimum post-oxidation annealing conditions are determined by changing the furnace temperature and annealing time. Compared with a unannealed laser device, the light output power increases by about 12%. An aging test is carried out to examine the reliability of the annealed oxide-confined VCSEL device. The temperature dependence of the lasing wavelength of the annealed oxide-confined VCSELs is also investigated.

OCIS codes: 250.5960, 250.7260, 140.7260.
doi: 10.3788/COL201210.122501.

Vertical-cavity surface-emitting lasers (VCSELs) are a relatively new class of semiconductor lasers. The novelty lies in their monolithic fabrication and surface-emitting feature[1]. The fabrication of VCSEL devices was first reported in 1979. Since then, VCSELs fabricated with etched pill, implanted, re-growth, and oxide-confined structures have been reported[2]. Among these structures, oxide-confined VCSELs have exhibited excellent performance, including such as high wall-plug efficiency, low threshold current, and high frequency modulation capability. These characteristics are due to the efficient optical mode and current confinement completed by the oxidation of AlAs or AlGaAs with abundant Al components[3]. The thermal selective wet oxidation confinement technique is widely used to fabricate infrared VCSELs such as 850 and 980 nm VCSELs[4,5]. Various papers have reported the control of thermal wet oxidation processing conditions[6,7]. Stable lateral oxidation is achieved by wet oxidation at 380–430 °C, and the oxide layer width can be determined by optical microscopy or scanning electron microscopy[8]. The wet oxidation process induces the formation of interface oxide traps, whose trap density has been investigated by a capacitance technique[9]. Post-oxidation annealing in a nitrogen environment at high temperatures can reduce the interface trap density and improve the characteristics of the device[10]. This kind of post-oxidation annealing can benefit oxide-defined VCSEL fabrication to improve the lasing performances. Indeed annealed 850 nm GaAs/AlGaAs VCSELs with an increase in light output power as high as 18% was reported[11]. However, to the best of our knowledge, the performance of the annealed VCSELs has not been detailed.

In this letter, the performance of 980-nm InGaAs/GaAs oxide-confined VCSELs subjected to post-oxidation annealing in a nitrogen environment at high temperatures was demonstrated. The optimum conditions for the post-oxidation annealing process were determined, and an approximately 12% increase in the light output power was observed. Given that the reliability of a laser device is also crucial to all laser device applications, an aging test was also conducted to examine the reliability of the annealed oxide-confined VCSELs. Finally, the temperature dependence of the lasing wavelength of the annealed VCSELs was also investigated.

VCSEL epitaxial wafers were grown on n^+-GaAs (100) substrates by low-pressure metal organic chemical vapour deposition. The schematic of the device structure is shown in Fig. 1(a). The active region had three $In_{0.2}Ga_{0.8}As$/GaAs quantum wells, and the emission wavelength of the device was designed to be about 980 nm. Two AlGaAs claddings were used to build the one-wavelength-thick cavity. The p-type distributed Bragg reflector (DBR) consisted of 35.5 pairs of $Al_{0.9}Ga_{0.1}As/Al_{0.12}Ga_{0.88}As$. A 30-nm-thick $Al_{0.98}Ga_{0.02}As$ layer was located between the active region and the p-type mirror. This layer was oxidized and converted to Al_xO_y in the process of realizeing carrier and optical confinement. The n-type DBR had only 25.5 pairs of $Al_{0.9}Ga_{0.1}As/Al_{0.12}Ga_{0.88}As$ to achieve bottom emission through the GaAs substrate.

Wet chemical etching was performed to define a 200-μm-diameter circular mesa. To form the current confinement aperture, thermal selective oxidation was carried out at furnace temperature 400 °C, N2 flow rate of 0.5 L/min, water bubbler temperature of 90 °C, and stable oxidation rate of 0.3 μm/min. A quartz tube furnace equipped with a resistance heater was used to control the process duration precisely. The oxidation depth into the mesa of the device was about 3 μm, and the oxide-aperture diameter was about 194 μm.

After oxidation, the surface of the sidewall of the mesa and the exposed active region were passivated with a Si_3N_4 passivation layer. The p-type Ti-Pt-Au contact on the top of the mesa was evaporated to serve as a metal pad for soldering. The GaAs substrate was thinned and polished down to about 130 μm to minimize its contribution to the series resistance, and an antireflection (AR) coating was deposited on the emission window. The

n-type Au-Ge-Ni electrical contact was deposited such that the emission window was surrounded. A thick Au layer was deposited on the top of the n-type electrical contact. The Au layer makes an ohmic contact with the substrate. Rapid thermal annealing was performed to reduce the metal contact resistance, and laser devices were tested under pulsed operation. To determine the optimum processing conditions, the laser devices were post-annealed in the furnace in a nitrogen environment at different furnace temperatures for different annealing durations.

The VCSELs operated at room temperature and under a pulsed condition with a pulse width of 50 μs and repeat frequency of 10 kHz. The measured emission spectrum of the device is shown in Fig. 1(b). The lasing peak wavelength is at 980.3 nm, and the full-width at half-maximum of the lasing spectrum is 0.8 nm.

Figure 2 shows the change in the light output peak power (in percentage values) of the devices at different post-oxidation annealing temperatures for 40 min. Post-oxidation annealing at low temperatures has little effect on the light output power change. Beyond 380 °C, the light output power then rapidly increases. Near 400–410 °C, the light output peak power improves. An increase (>10%) in the light output power is obtained after annealing at about 400 °C in a nitrogen environment. Thus annealing at about 400 °C is the optimum annealing temperature. Higher temperatures may have some negative effects on the metal contact in the device because the rapid thermal annealing temperature required to reduce metal contact resistance is about 410 °C. The increase in light output power can be attributed to the annealing of trapped charges in the oxide in the VCSEL mesa structures during the oxidation process[11]. Post-annealing oxidation was also carried out at 400 °C for different annealing time to determine the optimum duration, and the results are shown in Fig. 2 (inset). Light output power initially increases with the annealing time. After 40 to 60 min, the light output power begins to saturate. Therefore, the optimum conditions for post-annealing are 40 to 60 min and 400 °C.

The light output power-injection current ($L-I$) curves of an oxide-confined VCSEL before and after annealing at 400 °C for 40 min are shown in Fig. 3. The visible increase in light output peak power from the annealed device can be observed. The maximum light output power increases from 400 to 450 mW, which corresponds to an increase of about 12%. The maximum wall plug efficiency increases from the pre-annealing value of 9.6% to 11.2%, as shown in Fig. 3 (inset). The current-voltage characteristics of the annealed and unannealed devices

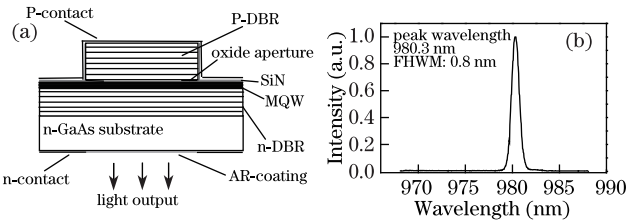

Fig. 1. (a) Schematic of the InGaAs/GaAs oxide-confined VCSEL device structure; (b) measured light emission spectrum.

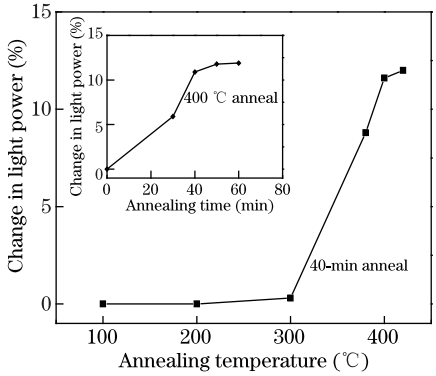

Fig. 2. Light output power change rate at different annealing temperatures. Inset: light output power change at 400 °C annealing temperature for different annealing time.

are also measured, and a slight voltage drop in the annealed device is observed. The threshold current decreases to 0.35 A from the pre-annealing value of 0.38 A. During wet oxidation, the formation of aluminum hydroxides is expected[12]. After annealing, most of the absorbed water evaporates, and the hydrogen concentration determined by the chemically bound H (in the form of aluminum hydroxides) can be strongly reduced. The interface charge density in the electrical confinement region is correspondingly reduced. Electron confinement is then significantly enhanced in the annealed lasers, resulting in reduced threshold current and improved output performance. Upon wet oxidation, stress buildup occurs due to the volume shrinkage of the high-Al-concentration layer. The thermal annealing process can relieve the stress between the oxide layer and the semiconductor materials when the samples are treated at high temperatures in a nitrogen atmosphere. Stress relaxation can result in better mechanical stability of the oxide-confined VCSELs.

The reliability of VCSEL devices is also very important in many practical applications. Therefore, an aging test was carried out to investigate the performance stability of the annealed oxide-confined InGaAs/GaAs VCSELs. We fabricated several VCSELs from the same wafer by the same procedure. Post-annealing process was carried out at 400 °C for 40 min. The devices were soldered onto a copper heat sink using an Au-Sn solder. For aging test, the devices were packaged and subjected to continuous wave (CW) operation at high temperatures. Figure 4 shows the results of the aging test of the randomly selected annealed oxide-confined InGaAs/GaAs VCSELs. During the test, the devices were driven under a constant current of 700 mA and the temperature was controlled at 70 °C. The values of the change in the light output power of the devices are shown in percentage in Fig. 4. No sudden power drop is observed during the entire aging test, and the total degradation of light output power is 7.1% on average after a 700-h test. After the aging test, the devices do not fail. Therefore, the improvement in the light output power via the post-oxidation annealing is reliable. Figure 4 (inset) shows the experimental results of the aging test of the unannealed oxide-confined VCSELs under the same operation conditions of 70 °C and 700-mA constant current. The total degradation is 8.2% on average, which is higher than the value of the annealed devices.

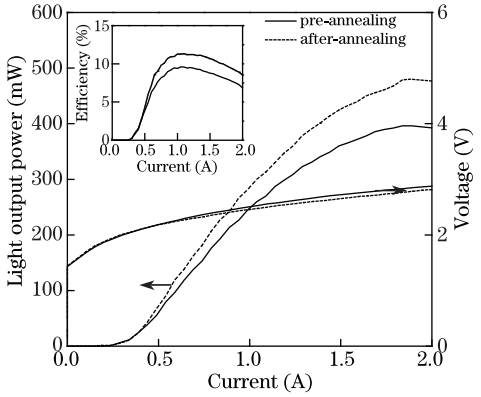

Fig. 3. Light output power-current and current-voltage characteristics of the device before and after annealing. Inset: wall plug efficiency of the device before and after annealing.

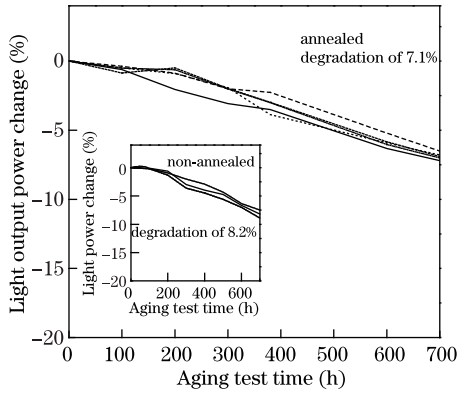

Fig. 4. Aging test of the annealed InGaAs/GaAs VCSELs. Inset: aging test of the unannealed lasers.

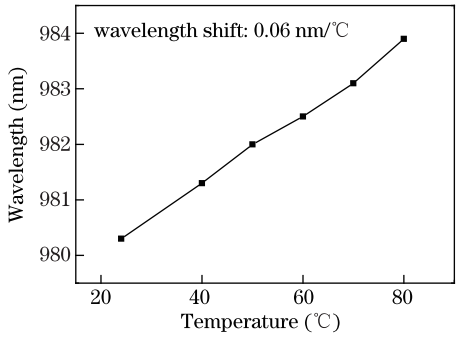

Fig. 5. Experimental temperature dependence of the lasing wavelength of the annealed InGaAs/GaAs VCSELs.

Finally, considering that wavelength stability is also important in device applications, the temperature dependence of the lasing wavelength of the annealed oxide-confined VCSELs was investigated by changing the device substrate temperature. The wavelength shift with temperature is about 0.06 nm/°C, as shown in Fig. 5. The shift rate is typical of VCSEL devices[13]. Therefore, the annealed VCSELs also show lasing wavelength stability.

In conclusion, InGaAs/GaAs VCSELs are fabricated by an oxidation confinement method, and the performance is improved by post annealing. Under the optimum conditions of 400 °C furnace temperature for 40 to 60 min, an approximately 12% increase in the light output power is obtained. This result can be attributed to the reduced interface charge intensity by heat treatment. An aging test of the annealed oxide-confined InGaAs/GaAs VCSELs reveals that the annealed device shows higher stability. The wavelength shift with temperature is also found to be about 0.06 nm/°C, which is typical of VCSEL devices. We believe that the annealing process can be widely used in VCSEL fabrication; AlAs (or AlGaAs with abundant Al components) oxide can be used as a carrier and optical confinement to improve the lasing performance. The oxidation apertures formed by the oxidation of AlAs may be more strained and thus be disadvantageous for the devices. Therefore, AlGaAs with abundant Al components are a good choice.

The authors gratefully acknowledge Dr. Qin Li of the Changchun Institute of Optics, Fine Mechanics, and Physics, Chinese Academy of Sciences for her helpful discussion. This work was supported by the National Natural Science Foundation of China under Grant Nos. 60676025 and 61076038.

References

1. R. S. Geels, S. W. Corzine, and L. A. Coldren, IEEE J. Quantum Electron. **27,** 1359 (1991).
2. W. W. Chow, K. D. Choquette, M. H. Crawford, K. L. Lear, and G. R. Haldey, IEEE J. Quantum Electron. **33,** 1810 (1997).
3. R. Jäger, M. Grabherr, C. Jung, R. Michalzik, G. Reiner, B. Weigl, and K. J. Ebeling, Electron. Lett. **33,** 330 (1997).
4. P. Westbergh, J. S. Gustavsson, B. Kögel, A. Haglund, A. Larsson, A. Mutig, A. Nadtochiy, D. Bimberg, and A. Joel, Electron. Lett. **46,** 1014 (2010).
5. A. Mutig, J. A. Lott, S. A. Blokhin, P. Wolf, P. Moser, W. Hofmann, A. M. Nadtochiy, A. Payusov, and D. Bimberg, Appl. Phys. Lett. **97,** 151101 (2010).
6. H. Q. Jia, H. Chen, W. C. Wang, W. X. Wang, W. Li, Q. Huang, and J. Zhou, Appl. Phys. Lett. **80,** 974 (2002).
7. H. Reese, Y. J. Chiu, and E. Hu, Appl. Phys. Lett. **73,** 2624 (1998).
8. M. Osinski, T. Svimonishvili, G. A. Smolyakov, V. A. Smagley, P. Mackowiak, and W. Nakwaski, IEEE Photonics Technol. Lett. **13,** 687 (2001).
9. N. C. Das, B. Gollsneider, P. Newman, and W. Chang, Appl. Phys. Lett. **81,** 1600 (2002).
10. P. D. Floyd and D. W. Treat, Appl. Phys. Lett. **70,** 2493 (1997).
11. N. C. Das and P. Newman, Solid-State Electron. **47,** 1359 (2003).
12. R. Todt, K. Dovidenko, A. Katsnelson, V. Tokranov, M. Yakimov, and S. Oktyabrsky, Mat. Res. Soc. Symp. Proc. **692,** 561 (2001).
13. Y. Sun, Y. Ning, T. Li, L. Qin, C. Yan, and L. Wang, J. Lumin. **122,** 886 (2007).